pISSN 1229-3008 eISSN 2287-6251
Progress in Superconductivity and Cryogenics
Vol.23, No.4, (2021), pp.19~24
https://doi.org/10.9714/psac.2021.23.4.019

Protection properties of HTS coil charging by rotary HTS flux pump in charging and compensation modes

Seunghak Han[a], Ji Hyung Kim[b], Yoon Seok Chae[b], Huu Luong Quach[b], Yong Soo Yoon[c], and Ho Min Kim[b, *]

[a] Department of Electrical and Electronic Engineering, Yonsei University, Seoul, South Korea
[b] Department of Electrical Engineering, Jeju National University, Jeju, South Korea
[c] Department of Electrical Engineering, Shin Ansan University, Ansan, South Korea

(Received 30 August 2021; revised or reviewed 5 November 2021; accepted 6 November 2021)

Abstract

The low normal zone propagation velocity (NZPV) of high-temperature superconducting (HTS) tape leads to a quench protection problem in HTS magnet applications. To overcome this limitation, various studies were conducted on HTS coils without turn-to-turn insulation (NI coils) that can achieve self-protection. On the other hand, NI coils have some disadvantages such as slow charging and discharging time. Previously, the HTS coils with turn-to-turn insulation (INS coils) were operated in power supply (PS) driven mode, which requires physical contact with the external PS at room-temperature, not in persistent current mode. When a quench occurs in INS coils, the low NZPV delays quench detection and protection, thereby damaging the coils. However, the rotary HTS flux pump supplies the DC voltage to the superconducting circuit with INS coils in a non-contact manner, which causes the INS coils to operate in a persistent current mode, while enabling quench protection. In this paper, a new protection characteristic of HTS coils is investigated with INS coils charging through the rotary HTS flux pump. To experimentally verify the quench protection characteristic of the INS coil, we investigated the current magnitude of the superconducting circuit through a quench, which was intentionally generated by thermal disturbances in the INS coil under charging or steady state. Our results confirmed the protection characteristic of INS coils using a rotary HTS flux pump.

Keywords: low normal zone propagation velocity, HTS coil, rotary HTS flux pump, quench protection, thermal disturbance

1. INTRODUCTION

The high-temperature superconducting (HTS) tape is a high current density wire suitable for applications requiring high energy density and high magnetic fields, such as NMR/MRI, maglev, tokamak and accelerator [1−7]. However, the low normal zone propagation velocity (NZPV), which is a fatal problem of the HTS tape, causes difficulties in quench detection and protection [8−12]. Without any detection and protection process, quench may cause permanent damage to HTS magnets; therefore, several studies have been conducted on quench detection and protection. Generally, the detect-and-dump and detect and-activate-heater protections has been suggested as active protection schemes for HTS magnets [13−17]. Moreover, the self-protecting behavior of no-insulation coils (NI coils), in which the insulation material between layers is completely eliminated, has been studied [18−24]. NI coils have the advantages of high electrical and thermal stabilities, and compact size. “However, the lack of turn-to-turn insulation in NI coils results in radial current flowing through turn-to-turn layers from its spiral current flowing along HTS wire due to very low contact surface resistance compared with INS coils. Thus, transport current from power source can be bifurcated and then response time of magnetic field is delayed on charging and discharging operations. The INS coils operated by the HTS flux pump may achieve the self-protecting feature similar to the NI coils, although the physical mechanism of thermal stability is completely different with NI coils under the transient state.

Generally, in conventional contact excitation system using the direct-current power supply (DC PS), the INS coils are operated by the current source mode of DC PS. The current source forcibly supplies current of constant magnitude, regardless of INS coil status, i.e., superconducting or normal states. Although fast the quench detection and power cut-off can protect the INS coils, the detection is difficult due to the slow NZPV of the HTS tape

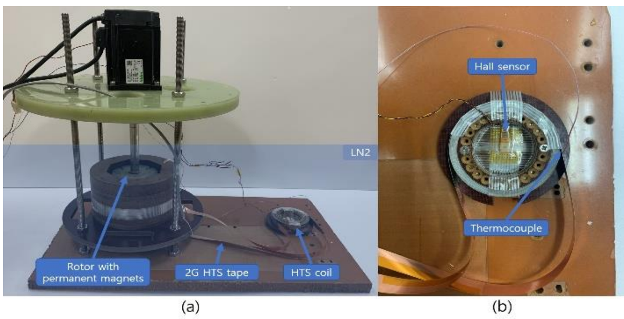

Fig. 1. Photographs of (a) basic structure of a rotary HTS flux pump and (b) HTS coil connected to the flux pump.

* Corresponding author: hmkim@jejunu.ac.kr

[25−29].

However, if the internal resistance increases once there is a quench occurrence, since HTS flux pump is a DC voltage source, the increased resistance obstructs the current creation in flux pump and current transfer inside the coil, leading to enabling self-protection for HTS coils. Additionally, since the flux pump is a non-contact excitation system, it is possible to not only eliminate the conduction loss through the current lead fundamentally but also to minimize the excitation loss generated in the current lead unlike the conventional contact excitation system [5], [31－36]. In this study, we experimentally investigated self-protection during quench occurrence in INS coil using a rotary HTS flux pump, which is one of the most active research topics among flux pumps.

2. EXPERIMENTAL SETUP

2.1. Rotary HTS flux pump

Fig. 1 (a) shows the basic structure of a rotary HTS flux pump, which consists of a second generation (2G) HTS tape physically connected for supplying the current to the HTS coil, and a rotor with permanent magnets (PMs) to generate an alternating magnetic field (AMF). When the rotor rotates, PMs pass through the width direction of 2G HTS tape. On the other hand, when an AMF is applied in the vertical direction, a voltage component called the open-circuit voltage (V_{oc}) is generated by Faraday's law [37－39]. The V_{oc} size varies over time and depends on the magnetic field size of the PM and the AMF passing frequency (f) [5, [34 － 36], 38]. The time varying V_{oc} (V_{oc}(t)) can be experimentally measured and is periodic. Fig. 2 (a) and (b) show the measured V_{oc}(t) and the DC voltage (V_{dc}) calculated by the V_{oc}(t), which is given by [40]:

$$V_{dc} = \frac{1}{T}\int_0^T V_{oc}(t)dt \quad (1)$$

where T is the AMF period of the HTS tape. As shown in Table I, we used SuNAM's 12 mm GdBCO copper CC to reduce the charging time and increase the maximum charging current [36]. The PM is N50 neodymium, which generates a magnetic field of about 0.21 T with HTS tape and 5 mm air-gap, which is large enough to render the HTS tape in a mixed state.

Depending on the magnitude of f, the average dc voltage (V), which is the actual voltage applied to the HTS coil during the unit time, is divided into low, mid, and high frequency ranges. Meanwhile, V_{oc}(t) varies in the frequency domain and should be used only at low frequency (f_{low}). In the experiment, we fixed eight PMs in the rotor, whose speed was increased from 100 rpm to 1000 rpm, with 100 rpm increments.

2.2. Structure of HTS coil

Fig. 1 (b) shows the HTS coil connected to the flux pump. As shown in Table I, the HTS coil was a double.
pancake, which was wound with turn-to-turn insulation using AMSC's 4.8 mm YBCO and Kapton. The critical current (I_c @77 K) and n-value of the HTS coil were 77.3 A and 39, respectively. Meanwhile, the inner diameter (ID) and outer diameter (OD) were 60 mm and 70.8 mm, respectively. The total length used was 8625 mm, while the inductance (L_{coil}) was 151.84 μH. A lakeshore cryogenic transverse hall sensor (HGCT-3020) was installed at the center of HTS coil to measure its generated magnetic field, while the current flowing through the HTS coil was calculated through the inverse calculation. The HTS coil temperature was measured by installing a lakeshore thermocouple (30 AWG, type E) on its OD.

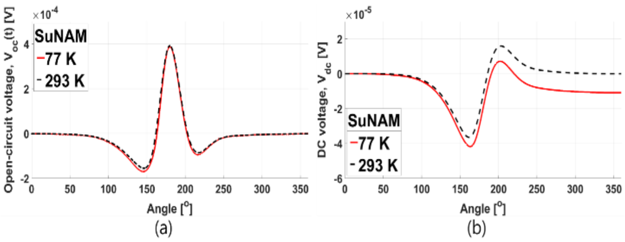

Fig. 2. Experimental results on (a) V_{oc}(t) and (b) calculated V_{dc} of SuNAM 12mm GdBCO CC at 77 and 293 K.

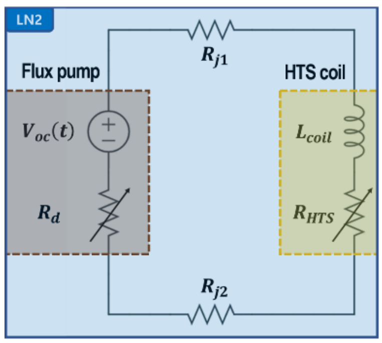

Fig. 3. Schematic of equivalent circuit with flux pump and HTS coil.

TABLE I
PARAMETERS OF HTS TAPE AND HTS COIL.

PARAMETERS	UNIT	VALUES	
Conductor	**Unit**	**Flux pump**	**Coil**
Manufacturer	-	AMSC	SuNAM
I_c @ 77 K, self-field	[A]	≥90	≥700
Width	[mm]	4.8	12
Thickness	[mm]	0.2075	0.15
HTS layer	-	YBCO	GdBCO
Cu stabilizer (both sides)	[μm]	50(laminated)	20(coated)
Substrate thickness	[μm]	75(Ni5W)	104(SUS)
HTS coil			
I_c @ 77 K	[A]	77.3	
Inner diameter (ID)	[mm]	60	
Outer diameter (OD)	[mm]	70.8	
Height	[mm]	12.3	
Turns (each layer)	-	20	
Kapton tape thickness	[mm]	0.0625	
Total length	[mm]	8625	
Inductance	[μH]	151.84	

2.3. Superconducting Equivalent Circuit

Fig. 3 demonstrates the superconducting equivalent circuit consisting of a flux pump. To create the thermal disturbance conditions in superconducting circuit, the HTS coil was intentionally exposed to room-temperature in this paper. The superconducting circuit used In-Bi to physically solder the flux pump and HTS coil. The solder generated joint resistance (i.e., $R_j = R_{j1}+R_{j2}$) was 298 nΩ. Meanwhile, the HTS coil resistance (R_{HTS}) changed according to temperature. In a liquid nitrogen (LN2) environment, the R_{HTS} can be simply assumed to 0 Ω while it increases sharply when temperature of HTS coil exceeds the critical temperature (T_c) of used HTS conductor. The T_c of AMSC YBCO was 93 K. Therefore, to generate quench on the HTS coil, as the purpose of this experiment, raising the temperature above 93 K becomes necessary. On the other hand, the AC loss occurred in the HTS tape by the flux pump AMF, while the resistance component was the dynamic resistance (R_d). To use the flux pump as an excitation device for HTS coils charging, V and R_d, parameters should be controlled, which increases along the second polynomial equation as the f of AMF increases. The R_d is calculated by [41]:

$$R_d = \frac{16a\Delta\phi}{I_{co}\pi D_{eff}}\left(1+\frac{2\Delta\phi}{\pi B_0 D_{eff}^2}\right)f = \beta f \quad (2)$$

where β is a constant defined by the design parameters of the rotary HTS flux pump, 2a is the width of the HTS tape, $\Delta\Phi$ is the total flux that passes across the HTS tape per rotor magnet crossing, I_{co} is the original critical current of the HTS tape, D_{eff} is the region that is fully penetrated by AMF in HTS tape, while B_0 is the relationship between I_{co} and the applied magnetic field within the HTS tape. The average dc voltage, V, is given by [36]:

$$V = V_{dc} f = I_{sat}R_T + L_{coil}\frac{dI_{sat}}{dt} \approx I_{sat}R_T \quad (3)$$

where I_{sat} is the saturation current flowing in the HTS coil. R_T is the total internal resistance of the superconducting circuit consisting of flux pump and HTS coil, which can be expressed as the summation of R_d, R_j, and R_{HTS}. The current magnitude at I_{sat} oscillates between increasing and decreasing, but exhibits a constant value at the macroscopic level. Therefore, the voltage generated by the HTS coil inductance can be regarded as zero.

3. RESULT AND DISCUSSION

Fig. 4 shows the charging current for the HTS coil using the rotary flux pump in steady state condition. The rotating speed (N_s) was increased from 100 to 1000 rpm, with 100 rpm increments. All experiments were performed in LN2. As the N_s increased, the I_{sat} magnitude increased and the charging time decreased. I_{sat} was charged up to 60−82% compared to I_c, which is summarized in Table II. To compare the charging time, the charging time constant (τ)

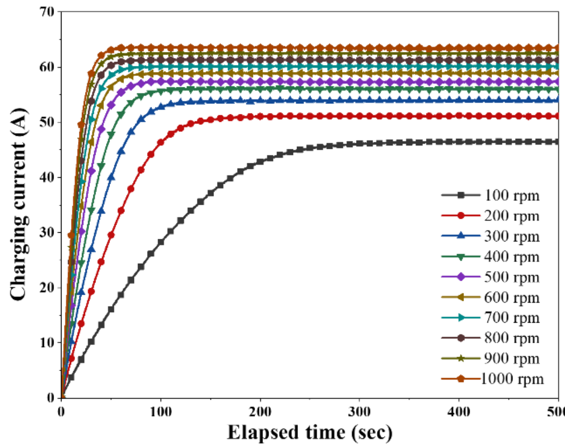

Fig. 4. Graph of charging HTS coil using a rotary flux pump in steady state.

TABLE II
EXPERIMENTAL RESULTS IN STEADY AND THERMAL DISTURBANCE STATE.

N_s [rpm]	I_{sat} [A]	I_{sat}/I_c [%]	V [μH]	τ [s]	R_d [μΩ]	R_d/R_j [%]	I_1 [A]	I_1/I_{sat} [A]
100	46	60	67	105	1.14	383	25	54
200	51	66	138	56	2.41	808	28	54
300	54	70	203	40	3.47	1164	30	56
400	56	73	270	32	4.52	1518	32	58
500	57	74	347	25	5.75	1930	31	55
600	59	76	412	22	6.70	2248	33	57
700	60	78	476	19	7.61	2554	35	59
800	61	79	538	17	8.48	2845	37	61
900	63	81	605	16	9.37	3145	38	61
1000	63	82	659	15	10.1	3390	38	61

corresponding to each N_s was measured, which was 105 − 15 s. The charging time constant, τ, can be expressed as

$$\tau = \frac{L_{coil}}{R_T} = \frac{L_{coil}}{R_d + R_j + R_{HTS}} \quad (4)$$

Here, the L_{coil} was 151.84 μH. Therefore, R_T can be calculated using L_{coil} and τ, while V can be calculated by equation (3). If V is expressed as the second polynomial equation for f, it can be expressed as V= -2.349×10$^{-9}f^2$+5.292×10^{-6}f. The R_j and R_{HTS} were 298 and 0 nΩ (in LN2), respectively. Calculating R_d from the equation. (4):

$$R_d = \frac{L_{coil}}{\tau} - \left(R_j + R_{HTS}\right) = \frac{151.84\times10^{-6}}{\tau} - 298\times10^{-9}(\Omega) \quad (5)$$

Calculated R_d from equation (5) was summarized in Table II and found to be around 3.83−33.90 times larger than R_j. If R_d is expressed as the second polynomial equation for f, it can be expressed as R_d= -1.305×10$^{-10}f^2$+9.351×10^{-8}f. These results confirmed that the charging time and I_{sat} were much more influenced by R_d than R_j.

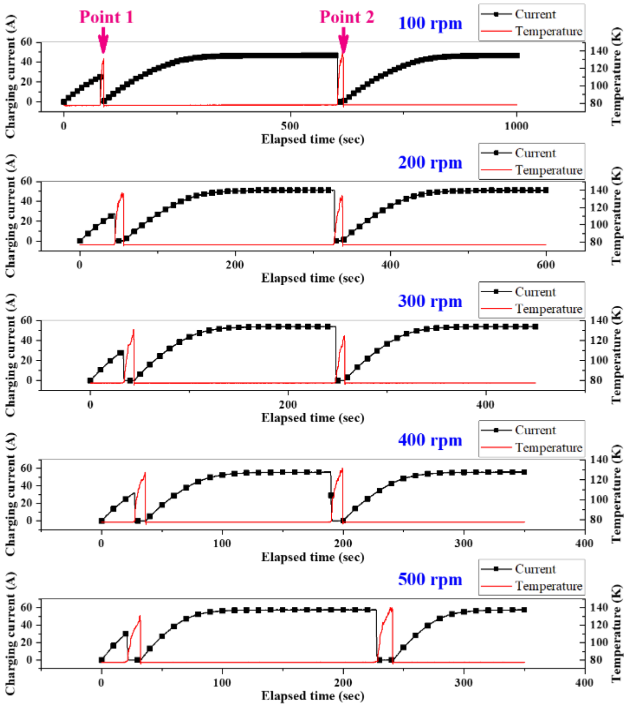

Fig. 5. Graphs of charged current and temperature of the HTS coil in the thermal quench at N_s = 100 to 500 rpm.

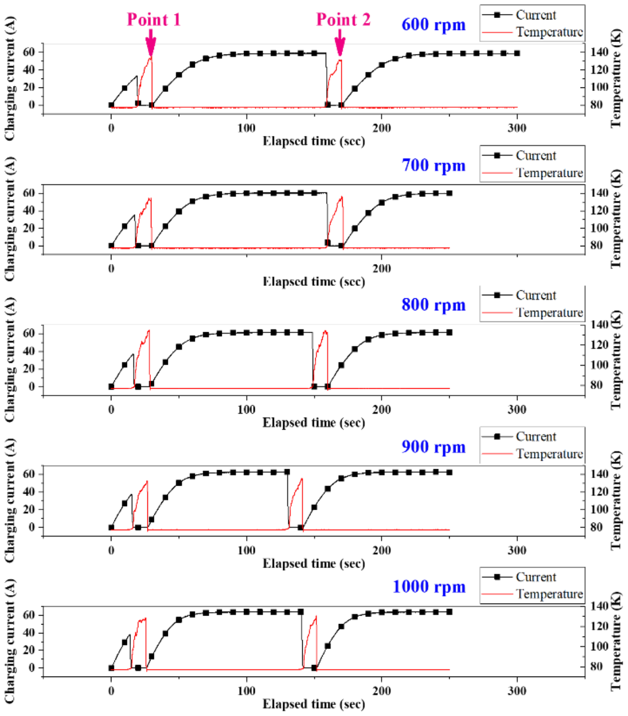

Fig. 6. Graphs of charged current and temperature of the HTS coil in the thermal quench at N_s = 600 to 1000 rpm.

Figs. 5 and 6 demonstrate the charged current and real-time temperature of the HTS coil with the quench in the charging and saturation states using the flux pump, which was taken out of LN2 to create thermal disturbances in the HTS coil. When quenching the HTS coil, the 12 mm HTS tape and N50 PMs of the flux pump continuously generated voltage in the LN2, which is the same process as the quench generation by taking it out of LN2 while charging the HTS coil using a common current source power supply. Points 1 and 2 generate quench in the charging and saturation states, respectively. To generate quench, the temperature of HTS coil was raised to 120−140K. The quench was generated at a similar ratio as much as possible compared to the I_{sat} at each rpm point. As summarized in Table II, the current ratio (i.e., $I_{ratio}=I_1/I_{sat}$) was about 54−61%. I_1 is the current at point 1. The current at point 2 generated the quench after confirming that the same current served as the saturation current using the flux pump was charged in the steady state without the quench generation. After the thermal quench, HTS coil was recharged and the charging speed and magnitude of I_{sat} were confirmed to be the same before and after the thermal quench. As a result, during the charging tests by flux pump, when quench occurred inside the HTS coil, the charged current automatically dissipated to protect the HTS coil from permanent damage because the flux pump is the voltage source. Existing current sources apply the same current amount even if the resistance increases due to quench in the HTS coil, leading to damage and destroy the HTS coil unless the power supply was cut off. Due to the low NZPV of the HTS tape, not only the detection is difficult, but also the protection process is complicated. However, if the thermal quench occurred during the HTS coil charging with the flux pump, flux pump can reduce the saturated current autonomously because current cannot be generated owing to not only no creation in V_{dc}, but also large increase in R_{HTS} at quench states. Thus, HTS coils can be protected from permanent damage even if the superconducting state are unstable. The current ripple, which is generated from the flux pump, causes magnetic field fluctuation. Therefore, it is difficult for utilizing in the applications that require high quality in magnetic field excitation, such as NMR, MRI, and accelerator magnets. However, the flux pump technique for HTS coil could be a promising method for enhancing the thermal stability of superconducting rotating machines because the current ripple does not affect insignificantly on the output quality of the rotating machine [42].

4. CONCLUSION

The quench detection in the HTS coil is difficult due to the low NZPV of the HTS tape. Therefore, research on quench detection is being actively conducted. The quench occurrence may damage the HTS coil if it was charged by a general current source. However, because the flux pump is a voltage source, when the HTS coil is quenched and the resistance is increased, the charged current is reduced by the resistance component; thus, the coil cannot be charged, leading to enabling self-protection. The HTS coil is recharged as it returns to a steady state. Although the HTS coils using flux pump shows high thermal stability, this technique may be limited for the applications requiring high quality of magnetic field because the current pulsation occurs during the charging state.

ACKNOWLEDGMENT

This work was supported by the National Research Foundation of Korea (NRF) grant funded by the Korea government (MSIT). (Nos. 2021R1C1C2003235 and 2019R1A2C1004715)

REFERENCES

[1] H. Maeda and Y. Yanagisawa, "Recent Developments in High-Temperature Superconducting Magnet Technology (Review)," *IEEE Trans. Appl. Supercond.*, vol. 24, no. 3, Jun. 2014, Art. no. 4602412.

[2] D. W. Hazelton *et al.*, "Recent developments in 2G HTS coil technology," *IEEE Trans. Appl. Supercond.*, vol. 19, no. 3, pp. 2218–2222, Jun. 2009.

[3] Y. S. Choi, D. L. Kim, and S. Y. Hahn, "Progress on the development of a 5 T HTS insert magnet for GHz class NMR applications," *IEEE Trans. Appl. Supercond.*, vol. 21, no. 3 PART 2, pp. 1644–1648, Jun. 2011.

[4] S. Lee *et al.*, "Persistent Current Mode Operation of A 2G HTS Coil with A Flux Pump," *IEEE Trans. Appl. Supercond.*, vol. 26, no. 4, Jun. 2016, Art. no. 0606104.

[5] Chris W Bumby *et al.*, "Development of a brushless HTS exciter for a 10kW HTS synchronous generator," *Supercond. Sci. Technol.*, vol. 29, no. 2, 2016, Art. no 024008.

[6] H. Jeon *et al.*, "PID Control of an Electromagnet-Based Rotary HTS Flux Pump for Maintaining Constant Field in HTS Synchronous Motors," *IEEE Trans. Appl. Supercond.*, vol. 28, no. 4, Jun. 2018, Art. no. 5207605.

[7] S. Han *et al.*, "Degradation of critical current in an HTS coated conductor considering curvature of ellipse for rotating flux pump," *Adv. Cryogenic Engr.*, vol. 89, pp. 141–146, Jan 2018.

[8] S. B. Kim, A. Saitou, J. H. Joo, and T. Kadota, "The normal-zone propagation properties of the non-insulated HTS coil in cryocooled operation," *Phys. C Supercond. its Appl.*, vol. 471, no. 21–22, pp. 1428–1431, 2011.

[9] S. B. Kim *et al.*, "The characteristics of the normal-zone propagation of the HTS coils with inserted Cu tape instead of electrical insulation," *IEEE Trans. Appl. Supercond.*, vol. 22, no. 3, Jun. 2012, Art. no. 4701504.

[10] D. Colangelo and B. Dutoit, "Impact of the normal zone propagation velocity of high-temperature superconducting coated conductors on resistive fault current limiters," *IEEE Trans. Appl. Supercond.*, vol. 25, no. 2, Apr. 2015, Art. no. 5601708.

[11] C. Lacroix and F. Sirois, "Corrigendum: Concept of a current flow diverter for accelerating the normal zone propagation velocity in 2G HTS coated" *Supercond. Sci. Technol.*, vol. 27, no. 12, 2014, Art. no. 035003.

[12] S. B. Kim *et al.*, "The study on improving the self-protection ability of HTS coils by removing the insulation and lamination of the various metal tapes," *Phys. C Supercond. its Appl.*, vol. 484, pp. 310–315, 2013.

[13] Y. Iwasa, *Case Studies in Superconducting Magnets: Design and Operational Issues*, 2nd ed. New York, NY, USA: Springer-Verlag, 2009, pp. 496–505.

[14] Y. Iwasa *et al.*, "Stability and quench protection of coated YBCO 'composite' tape," *IEEE Trans. Appl. Supercond.*, vol. 15, no. 2, pp. 1683–1686, Jun. 2005.

[15] S. Hahn *et al.*, "A 78-mm/7-T multi-width no-insulation ReBCO magnet: Key concept and magnet design," *IEEE Trans. Appl. Supercond.*, vol. 24, no. 3, Jun. 2014, Art. no. 4602705.

[16] W. Yao, J. Bascunan, S. Hahn, and Y. Iwasa, "MgB_2 coils for MRI applications," *IEEE Trans. Appl. Supercond.*, vol. 20, no. 3, pp. 756–759, Jun. 2010.

[17] J. H. Kim *et al.*, "Effects of stabilizer thickness of 2G HTS wire on the design of a 1.5-MW-class HTS synchronous machine," *IEEE Trans. Appl. Supercond.*, vol. 26, no. 4, Jun. 2016, Art. no. 5206705.

[18] S. Hahn, D. K. Park, J. Bascuñán, and Y. Iwasa, "HTS pancake coils without turn-to-turn insulation," *IEEE Trans. Appl. Supercond.*, vol. 21, no. 3, pp. 1592–1595, Jun. 2011.

[19] Y. G. Kim, S. Hahn, K. L. Kim, O. J. Kwon, and H. G. Lee, "Investigation of HTS racetrack coil without turn-to-turn insulation for superconducting rotating machines," *IEEE Trans. Appl. Supercond.*, vol. 22, no. 3, Jun. 2012, Art. no. 5200604.

[20] H. J. Shin et al., "A study on cooling performances and over-current behaviors of GdBCO coils with respect to epoxy impregnation method," *IEEE Trans. Appl. Supercond.*, vol. 25, no. 3, Jun. 2015, Art. no. 4602105.

[21] S. Hahn et al., "No-insulation coil under time-varying condition: Magnetic coupling with external coil," *IEEE Trans. Appl. Supercond.*, vol. 23, no. 3, Jun. 2013, Art. no. 4601705.

[22] Y. H. Choi, S. G. Kim, S. H. Jeong, J. H. Kim, H. M. Kim, and H. Lee, "A Study on Charge-Discharge Characteristics of No-Insulation GdBCO Magnets Energized via a Flux Injector," *IEEE Trans. Appl. Supercond.*, vol. 27, no. 4, Jun. 2017, Art. no. 4601206.

[23] K. L. Kim et al., "Analytical and empirical studies on the characteristic resistances of no-insulation GdBCO racetrack pancake coil under various operating currents," *Curr. Appl. Phys.*, vol. 15, no. 1, pp. 8–13, Jan. 2015.

[24] Y. H. Choi et al., "Thermal quench behaviors of no-insulation coils wound using GdBCO coated conductor tapes with various lamination materials," *IEEE Trans. Appl. Supercond.*, vol. 24, no. 3, Jun. 2014, Art. no. 8800105.

[25] H. Song, K. Gagnon, and J. Schwartz, "Quench behavior of conduction-cooled y Ba2Cu3O 7-δ coated conductor pancake coils stabilized with brass or copper," *Supercond. Sci. Technol.*, vol. 23, no. 6, 2010, Art. no. 065021.

[26] L. A. Angurel *et al.*, "Quench detection in YBa2 Cu3 O7-δ coated conductors using interferometric techniques," *J. Appl. Phys.*, vol. 104, no. 9, Nov. 2008, Art. no. 093916.

[27] S. Liu, L. Ren, J. Li, and Y. Tang, "Analysis of quench propagation characteristics of the YBCO coated conductor," *Phys. C Supercond. its Appl.*, vol. 471, no. 21–22, pp. 1080–1082, 2011.

[28] H. Y. Park *et al.*, "Analysis of temperature dependent quench characteristics of the YBCO coated conductor," *IEEE Trans. Appl. Supercond.*, vol. 20, no. 3, pp. 2122–2125, Jun. 2010.

[29] D. Uglietti and C. Marinucci, "Design of a quench protection system for a coated conductor insert coil," *IEEE Trans. Appl. Supercond.*, vol. 22, no. 3, Jun. 2012, Art. no. 4702704.

[30] H. Jeon *et al.*, "Methods for Increasing the Saturation Current and Charging Speed of a Rotary HTS Flux-Pump to Charge the Field Coil of a Synchronous Motor," *IEEE Trans. Appl. Supercond.*, vol. 28, no. 3, Apr. 2018, Art. no. 5202605.

[31] H. Jeon *et al.*, "PID Control of an Electromagnet-Based Rotary HTS Flux Pump for Maintaining Constant Field in HTS Synchronous Motors," *IEEE Trans. Appl. Supercond.*, vol. 28, no. 4, Jun. 2018, Art. no. 5207605.

[32] C. Hoffmann, D. Pooke, and A. D. Caplin, "Flux pump for HTS magnets," *IEEE Trans. Appl. Supercond.*, vol. 21, no. 3, pp. 1628–1631, Jun. 2011.

[33] A. E. Pantoja, Z. Jiang, R. A. Badcock, and C. W. Bumby, "Impact of Stator Wire Width on Output of a Dynamo-Type HTS Flux Pump," *IEEE Trans. Appl. Supercond.*, vol. 26, no. 8, Dec. 2016, Art. no. 4805208.

[34] Z. Jiang, C. W. Bumby, R. A. Badcock, H. J. Sung, and R. A. Slade, "A novel rotating HTS flux pump incorporating a ferromagnetic circuit," *IEEE Trans. Appl. Supercond.*, vol. 26, no. 2, Mar. 2016, Art. no. 4900706.

[35] S. Lee *et al.*, "Persistent Current Mode Operation of A 2G HTS Coil with A Flux Pump," *IEEE Trans. Appl. Supercond.*, vol. 26, no. 4, Jun. 2016, Art. no. 0606104.

[36] S. Han *et al.*, "Charging Characteristics of Rotary HTS Flux Pump with Several Superconducting Wires," *IEEE Trans. Appl. Supercond.*, vol. 29, no. 5, Aug. 2019, Art. no. 0603605.

[37] H. Jeon et al., "Methods for increasing the saturation current and charging speed of a rotary HTS flux-pump to charge the field coil of a synchronous motor," *IEEE Trans. Appl. Supercond.*, vol. 28, no. 3, Apr. 2018, Art. no. 5202605.

[38] C. W. Bumby, Z. Jiang, J. G. Storey, A. E. Pantoja, and R. Badcock, "Anomalous open-circuit voltage from a high-Tc superconducting dynamo," *Appl. Phys. Lett.*, vol. 108, 2016, Art. no. 122601.

[39] Z Jiang, C. W. Bumby, R. A. Badcock, H.-J. Sung, N. J. Long, and N. Amemiya, "Impact of flux gap upon dynamic resistance of a rotating HTS flux pump," *Supercond. Sci. Technol.*, vol. 28, no. 11, Sep. 2015, Art. no. 115008.

[40] J. Geng et al., "Origin of dc voltage in type II superconducting flux pumps: Field, field rate of change, and current density dependence of resistivity," *J. Phys. D, Appl. Phys.*, vol. 49, no. 11, 2016, Art. no. 11LT01.

[41] Z. Jiang, K. Hamilton, N. Amemiya, R. A. Badcock, and C. W. Bumby, "Dynamic resistance of a high-Tc superconducting flux pump," *Appl. Phys. Lett*., vol. 105, 2014, Art. no. 112601.

[42] J. H. Kim *et al*., "Fabrication and performance testing of a 1-kW-high-temperature superconducting generator with a high-temperature superconducting contactless field exciter," *Supercond. Sci. Technol*., vol. 33, Jul. 2020, Art. no. 095003.